Journal of Materials Chemistry

Cite this: J. Mater. Chem., 2011, 21, 17881

www.rsc.org/materials

PAPER

Controlled carboxylic acid introduction: a route to highly purified oxidised single-walled carbon nanotubes†

Kevin Flavin,[a] Ilona Kopf,[a] Elisa Del Canto,[a] Cristina Navio,[b] Carla Bittencourt[b] and Silvia Giordani*[a]

Received 18th May 2011, Accepted 14th September 2011
DOI: 10.1039/c1jm12217g

A chemical treatment for preparing high purity selectively oxidised SWNTs while preserving optical/electronic properties of the material has been developed. Efficient removal of both metal and carbonaceous impurities has been demonstrated by AFM, TEM, Raman and absorption spectroscopy, while XPS confirmed quantitative conversion of oxidised defects to functionalisable carboxylic acid groups. Furthermore persistence of the characteristic optical properties was confirmed using absorption and NIR photoluminescence spectroscopy, thus indicating preservation of the electronic structure. This chemical treatment thus paves the way for the preparation of high purity, covalently functionalised SWNTs enhancing their potential for use in high-performance optical/electronic applications. A comparison with commonly used purification protocols that utilize nitric acid and sodium hydroxide followed by piranha solution treatments or simple solvent washing is made, highlighting the advantages of the reported method for the production of SWNT starting materials ideal for efficient chemical modifications.

Introduction

Single-walled carbon nanotubes (SWNTs) display very unique electrical, optical, thermal, and mechanical properties, resulting from the highly conjugated electronic structure which they possess. However, widespread exploitation of these materials for high-performance applications has to date been impeded by inadequate purity, solubility and processability. Chemical treatment[1–13] and functionalisation[14–18] of SWNTs are seen among the most plausible methods for overcoming these problems and driving toward the production of more manageable multifunctional materials.[18,19] The most common approach relies on the oxidative treatment of the sample with nitric acid,[1,3,5–9,20] which has the dual role of dissolving the catalyst nanoparticles and introducing oxidised defects onto the SWNTs, of which the carboxylic acid groups may be functionalised using amidation or esterification reactions.[12,21]

There are however a number of limitations associated with the nitric acid treatment process. Firstly, it destroys the SWNTs converting them to carbonaceous impurities over time. Haddon and co-workers have demonstrated that, even under the mildest conditions, only 34% of the sample is present as SWNTs following this oxidative treatment.[5] Secondly, the nitric acid treatment produces a variety of oxygenated defect sites on the SWNTs, ranging from alcohols and ethers to aldehydes and ketones in addition to carboxylic acids, which is inefficient as coupling reactions only occur with the latter.[6,12] Finally, defects that are introduced onto the SWNTs during the nitric acid treatment are produced by conversion of sp^2 to sp^3 hybridised carbon, which damages the electronic structure of the SWNTs and hence affects the extraordinary electronic and optical properties which they possess.[9]

In recent years, a number of reports have investigated the removal of carboxylic acid containing carbonaceous impurities, through conversion of the acid groups to their more soluble sodium salts, by treatment with sodium hydroxide.[4,10,11,13,22,23] Although highly effective this procedure does not address either the problem of carbonaceous impurities that do not contain carboxylic acid groups, or the wide variety of oxygen containing functional groups present in the sample. The effect of sodium hydroxide treatment on a two step purification/oxidation procedure was more recently investigated, and it was demonstrated that the use of a second oxidation step aided in the conversion of defects to reactive carboxylic acid groups.[2] Considering this, the key to this work lies in the development of a mild oxidation step, which allows complete conversion of defect sites to carboxylic acid groups, and therefore should allow both efficient functionalisation and the possibility of completely removing all carbonaceous impurities with minimal damage to the electronic structure of the SWNTs.

In this article we report a chemical treatment protocol (Scheme 1) that has been developed for the preparation of high

[a]Trinity College Dublin, School of Chemistry/CRANN, College Green, Dublin 2, Ireland. E-mail: giordans@tcd.ie; Fax: +353 (0)1 896 1422; Tel: +353 (0)1 671 2826
[b]University of Mons, ChiPS, Parc Initialis, Av. Nicolas Copernic 1, Mons, 7000, Belgium

† Electronic supplementary information (ESI) available: Supplementary TEM, FTIR and Raman spectra, in addition to XPS and NIRPL data. See DOI: 10.1039/c1jm12217g

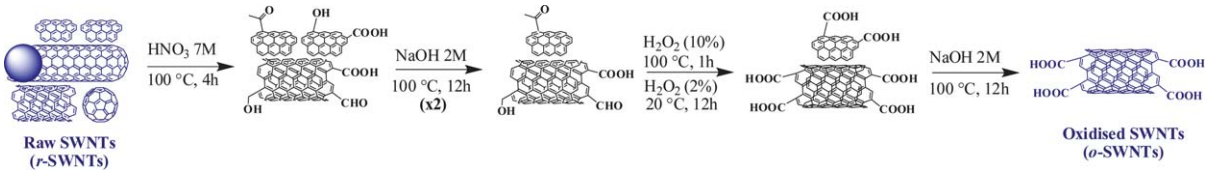

Scheme 1 Purification/oxidation protocol.

purity oxidised SWNTs, where highly efficient removal of carbonaceous impurities and conversion of oxidised defects to carboxylic acid groups is demonstrated. The comparison of this purification/oxidation protocol with commonly used method that employs nitric acid and sodium hydroxide[2,4,10,20,23] followed by treatment with piranha solution,[2] which is a mixture of sulphuric acid and hydrogen peroxide (Scheme S1†), highlights the key role of hydrogen peroxide in the efficient etching of residual carbonaceous impurities and in the oxidation of the tubes' defect sites. Furthermore, we demonstrate the persistence or even enhancement of the characteristic optical properties of the SWNTs, thus paving the way for the preparation of high purity, covalently functionalised SWNTs with relatively unimpaired electronic properties and hence enhancing their potential for use in high-performance optical/electronic applications.

Experimental

Materials

SWNTs produced by the HiPco technique were purchased from Unidym®, Inc. (Lot no. R1912/R0513). Reagents and solvents were purchased as reagent-grade from Fisher Scientific Ireland Ltd, or Sigma-Aldrich Ireland and used without further purification.

Nitric acid treatment. Typically a 100 mg quantity of r-SWNTs was dispersed in 7 M HNO_3 (340 ml) by sonication for 5 min (150 W) and subsequently for 10 min (50 W). The mixture was then stirred under reflux at 100 °C for 4 h‡ and quenched with 500 g of ice. The dispersion was then filtered through a Millipore system (0.2 μm Isopore™ filter) and washed with distilled water until the filtrate ran neutral. Following neutralisation the sample was washed with a further 2 L of distilled water, never allowing the solid to dry.

Sodium hydroxide treatment. The wet solid was transferred directly from the Millipore filter to a Teflon® tub, dispersed in 200 ml of 2 M NaOH by sonication for 5 min (150 W) and subsequently stirred overnight at 100 °C under a nitrogen atmosphere. The mixture was cooled to room temperature, filtered through over an Isopore™ filter and washed with a further 200 ml of 2 M NaOH. The solid was washed with distilled water until the filtrate pH became neutral and the sample was subjected to the NaOH treatment one additional time. Following neutralisation the sample was washed with a further 2 L of distilled water, again never allowing the solid to dry.

‡ The length of time which the r-SWNTs are refluxed in nitric acid should be altered based on the quantity of catalyst present in the raw material. We suggest 4 h for samples with approximately 30% catalyst; however 6 h or longer is suggested for samples containing ≥40%.

Hydrogen peroxide treatment. Following filtration the wet solid was dispersed in 200 ml of 10% H_2O_2 by sonication for 5 min (150 W) and subsequently refluxed for 1 h at 100 °C. The dispersion was quenched with 800 g of ice (diluting to 2% H_2O_2) and allowed to stand for 12 h. The dispersion was filtered over an Isopore™ filter and washed with copious amounts of distilled water (never allowing sample to dry).

Sodium hydroxide treatment. The wet solid was again transferred directly to a Teflon® tub, dispersed in 200 ml of 2 M NaOH and refluxed under a nitrogen atmosphere (as above). The mixture was again washed with 200 ml of 2 M NaOH, with distilled water until the filtrate pH became neutral, a further 2 L of distilled water, 200 ml of 1 M HCl and finally with copious amounts of water after filtrate pH became neutral. Yields of 15–23% were achieved depending on the quantities of catalyst and carbonaceous impurities present in the raw material.

Nitric acid/sodium hydroxide treatment. A 300 mg quantity of r-SWNTs was dispersed in 2.6M HNO_3 (300 ml) by sonication. The mixture was stirred under reflux at 100 °C for 48 h and cooled down to room temperature. The dispersion was then filtered through a Millipore system (0.2 μm Isopore™ filter) and washed with distilled water until the filtrate ran neutral. Following neutralisation the sample was dispersed in DMF (100 mL) by sonication for 30 min, and washed with DMF (500 mL) until the filtrate ran clear. The sample was re-suspended in NMP (100 mL), sonicated for 60 min and filtered on a 0.2 μm Millipore Fluoropore™ membrane. After careful washing with NMP (100 mL), DMF (200 mL) and MeOH (200 mL) respectively, the sample was collected, dispersed in water (100 mL), sonicated for 60 min and freeze dried. A 100 mg quantity of the nitric acid treated sample was dispersed in 100 mL of 8 M NaOH by sonication for 30 min, and subsequently stirred at 100 °C for 48 h in a Teflon® tub under a nitrogen atmosphere. The mixture was cooled to room temperature, filtered through over a 0.2 μm Isopore™ filter and washed with deionised water (3L) until neutral pH was reached. The basic treatment was repeated two additional times on the residue left on the filter. Yield 55%.

Piranha solution treatment. SWNTs were shortened and oxidised with a mixture of sulphuric acid and hydrogen peroxide following a previously reported procedure.[2]

Sample characterisation

AFM topographic images were collected in semi-contact mode with an NT-MDT NTEGRA Spectra inverted configuration system. Silicon tips with reflectance gold coated on the back, tip apex radius 10 nm, force constant 2 N m^{-1} and frequency 170 kHz were used. The data were collected with NT-MDT Nova

software and analysed with Gwyddion and WSxM SPM freeware.[24] Samples were prepared by dispersing the nanotubes in high purity DMF by sonication, spray coating them onto freshly cleaved mica substrates and drying them overnight in the oven at 100 °C. For the length distribution analysis, samples were dispersed at lower concentration in order to adequately estimate single nanotube length. Statistical analysis was performed on samples of 100 SWNTs. The contour length of individual SWNTs was measured using the segmented line profiling tool from WSxM SPM freeware.[24]

TEM measurements were performed with a FEI Titan 80–300 operated at 300 kV, where samples were prepared by drop coating SWNT dispersions in DMF onto a lacey carbon coated 400 mesh copper grid.

XPS measurements were performed in a VERSAPROBE PHI 5000 from Physical Electronics, equipped with a Monochromatic Al K_α X-Ray source with a highly focused beam size which can be selected from 10 μm to 300 μm. The energy resolution was 0.6 eV. For the compensation of built up charge on the sample surface during the measurements a dual beam charge neutralisation composed of an electron gun (~1 eV) and the Argon Ion gun (≤10 eV) was used.

Micro-Raman scattering measurements were performed at room temperature in the backscattering geometry using RENISHAW 1000 micro-Raman system equipped with a CCD camera and a Leica microscope. An 1800 lines mm^{-1} grating was used for all measurements, providing a spectral resolution of ±1 cm^{-1}. As excitation sources an Ar^+ laser (514 nm) and a HeNe laser (633 nm) were used. Measurements were taken with 10 s of exposure time and 4 accumulations. The laser spot was focused on the sample surface using a 50x objective with short-focus working distance. Raman spectra were collected on numerous spots on the sample and recorded with Peltier cooled CCD camera. The data was collected and analysed with Renishaw Wire and GRAMS software.

Absorption spectroscopy was carried out on a PerkinElmer UV-Vis/NIR Lambda 1050 Absorption Spectrophotometer. All spectra were recorded on supernatants after 1 cycle, with an interval of 1 nm, slit width 2 nm and scan speed of 240 nm min^{-1}. Samples were either dispersed in NMP or aqueous SDBS by sonication (3–4 h at medium power) and measurements were carried out in a 1 cm quartz cell on the dispersion supernatant following centrifugation at 8000 RPM (900 × g) for 90 min (to remove aggregates and large bundles).

NIR photoluminescence studies were carried out in a L.O.T. ORIEL Nanospectralyzer NS1 at three different excitation wavelengths (785, 683 and 638 nm). Dispersions of SWNTs in aqueous SDBS were prepared in D_2O with an initial nanotubes concentration of 2×10^{-2} mg ml^{-1} and with a SWNTs/SDBS mass ratio of 1 : 25. Nanotubes and SDBS were precisely weighted and dispersed in D_2O water by both sonic tip (2 min) and sonic bath (3–4 h) treatments. The dispersions were centrifuged at 8000 rpm for 90 min and all optical measurements were carried out on the supernatants in a 1 cm quartz cells.

TGA analyses were carried out on samples using a PerkinElmer Thermogravimetric Analyzer Pyris 1 TGA. The method used for recording the TGA measurements in air flow was: 1) hold for 5 min at 30 °C; 2) heat from 30 °C to 100 °C at 10 °C min^{-1}; 3) hold for 20 min at 100 °C; 4) heat from 100 °C to 900 °C at 10 °C min^{-1}.

FTIR spectra were measured in the solid state on a Perkin-Elmer FTIR Spectrometer Spectrum 100 with a universal ATR sampling accessory (diamond/ZnSe crystal). Spectra for were recorded at 36 and 256 scans, respectively, with a 4 cm^{-1} resolution.

Results and discussion

Initially a portion of raw HiPco SWNTs (r-SWNTs) was refluxed in 7 M nitric acid for 4 h (Scheme 1). A short reaction time was chosen to minimise the damage sustained by the SWNTs, while removing a large fraction of the catalyst impurity.[5] The sample was subsequently refluxed in 2 M sodium hydroxide, which allowed the removal of the carboxylated fraction of the carbonaceous impurities (by conversion to the more soluble salt) as previously reported by Green and co-workers.[10] The sample was then subjected to a second oxidation step which consisted of refluxing in 10% hydrogen peroxide for 1 h followed by diluting/quenching with ice and allowing to stand for 12 h. This step etches away remaining carbonaceous impurities and quantitatively converts oxygenated defects to carboxylic acid moieties. Here the use of a strong acid was avoided to overcome any further damage/decomposition of the SWNTs and prevent production of additional carbonaceous impurity.[2] Any remaining carbonaceous impurities (carboxylated during the second oxidation step) were removed through a final sodium hydroxide treatment, yielding highly purified selectively oxidised SWNTs (o-SWNTs). Another portion of raw HiPco SWNTs was subjected to a liquid phase purification protocol firstly reported by Smalley and co-workers and still widely used by the nanotube community, which consists of refluxing the nanotubes in 2.6 M nitric acid for 48 h.[7,25–28] Following 8 M sodium hydroxide treatment the removal of carboxylated carbonaceous fragments was ensured,[10] yielding HNO_3/NaOH treated SWNTs (b-SWNTs). Purity and properties of o-SWNTs was investigated by using a variety of complementary spectroscopic and microscopic techniques, and a direct comparison to that of b-SWNTs was made throughout the article. Additional comparison to previously reported HNO_3/NaOH treated SWNTs followed by treatment with piranha solution,[2] here referred as oo-SWNTs, was also reported.

Purity of the SWNTs was evaluated by AFM and TEM (Fig. 1 and Fig. 2), where samples were dispersed in DMF by sonication and sprayed directly onto the substrate. Further sample pre-treatment such as centrifugation was avoided as this tends to enhance the apparent purity of the sample. Efficient removal of impurities (Figure S1†) is evident in comparison of AFM images taken before and after chemical treatment (Fig. 1), where the r-SWNT sample is dominated by carbonaceous and metal based impurities (single dots), while the o-SWNT sample is comprised almost entirely of small SWNT bundles. When topographic images of o-SWNTs and b-SWNTs are compared (Figure S2†), the persistence of small dots in the latter is clearly observable. This, besides the number of AFM images reported in the literature where carbonaceous fragments are visible after purification and acid treatment,[2,4,29–31] is an indication of the efficacy of the second oxidation step in converting carbonaceous impurities to easily NaOH washable fragments. Analysis of the length distribution demonstrated only a small reduction in the average length

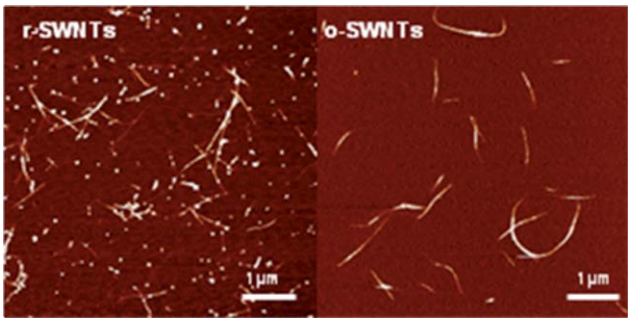

Fig. 1 AFM images of raw and oxidised SWNTs. Z-heights for the AFM images of raw SWNTs 0–5 nm and for the oxidised SWNTs 0–10 nm.

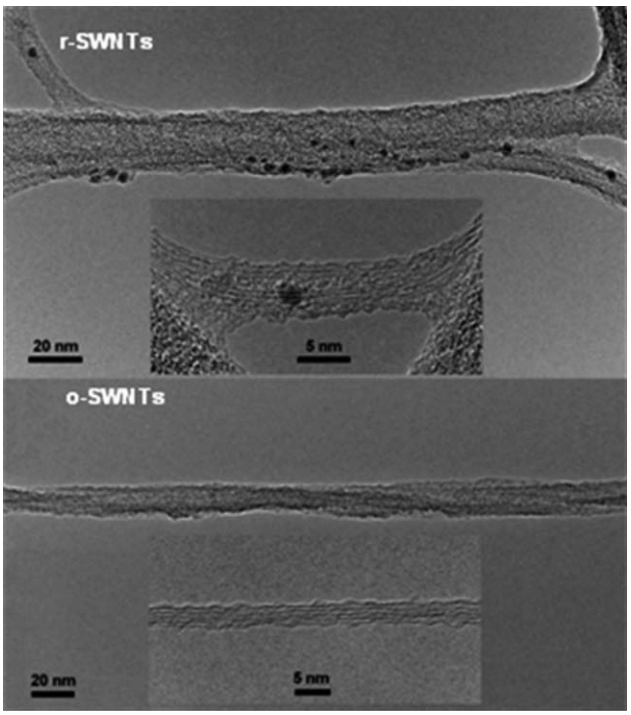

Fig. 2 HRTEM images of raw and oxidised SWNTs.

from 437 to 388 nm in comparison of the raw and oxidised samples, respectively (Figure S3†). HRTEM (Fig. 2) also demonstrates the effective removal of the catalyst nanoparticles (black dots) during the chemical treatment, while integrity of the nanotube structure is maintained (inset o-SWNTs). The homogeneity of this treatment is however more clearly evident from images of larger areas reported in Figure S4.† Results from TGA (Figure S5†) are in agreement demonstrating a reduction in the residue remaining, from approximately 30 to 2% (which may also include salts produced during acid base neutralisation). This is accompanied by an increase in the main graphitic decomposition temperature from 460 to 575 °C, indicating removal of the metal impurity, which causes pre-combustion of the SWNTs due to thermal oxidation.[32] A contribution to the above mentioned up-shift can be also attributed to the clearing of carboxylated fragments from base washed nitric acid treated SWNTs.[13] When TGA first derivative curves of r-SWNTs and b-SWNTs are compared (Figure S5B†) an increase of ~10 °C in the combustion temperature of the nanotube component is recorded. This is in agreement with what previously reported by Haddon and co-workers,[13] that showed an up-shift of ~20 °C after removal of carboxylated carbonaceous impurities. However, following the purification/oxidation protocol here proposed, the temperature up-shift extent is much more significant (>100 °C), thus confirming the improved purity of o-SWNTs.

Changes in the nature of the functional groups present in the sample following the chemical treatment process were monitored by XPS. The C 1s core level spectra for the raw and oxidised SWNTs as well as that of HNO_3/NaOH treated SWNTs are illustrated in Fig. 3. Each spectrum is reproduced by fitting it into its various components and as expected characteristic contributions including the primary graphitic peak (284.4 eV) and plasmon loss (290.6 eV) are evident for the r-SWNTs. The spectrum of the o-SWNTs (Fig. 3), however, only displays two new peaks *i.e.* the "defect" peak (285.3 eV) produced by conversion of sp^2 to sp^3 hybridised carbon and the carboxyl peak (288.8 eV). This implies that the second oxidative step results in practically quantitative conversion of the oxidised defects to carboxylic acid groups (Table S1†), yielding a material ideal for efficient further chemical modifications. The functional composition of o-SWNTs is even more appreciable when XPS data are compared to that of b-SWNTs, which display additional

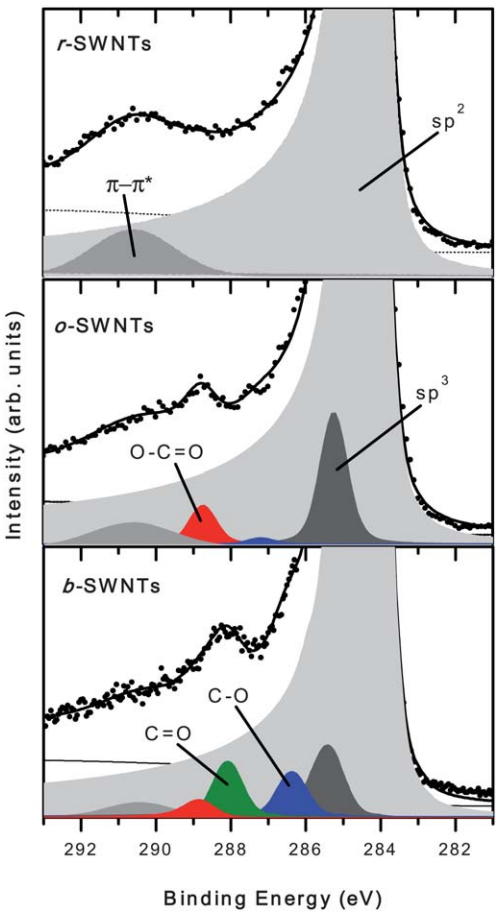

Fig. 3 XPS C 1s spectrum of raw and oxidised SWNTs compared to a typical sample after HNO_3/NaOH treatment.

contributions of less oxidised states of carbon such as carboxyl, carbonyl, aldehyde, alcohol and ether between 284.5 and 288.8 eV (Fig. 3 and Table S1†).[6,26] When XPS data of o-SWNTs are compared to that of previously reported 2-step oxidised oo-SWNTs,[2] the contribution of carbonyl and alcohol functional groups is quantitatively comparable in the latter. This confirms the more effective conversion of oxidised defects to carboxylic acid groups following the purification/oxidation protocol presented here. FTIR analysis of the samples following the purification/oxidation chemical treatment shows the appearance of broad O–H (3000–3600 cm^{-1}) and C=O (~1625 and 1725 cm^{-1}) stretches (Figure S6†).[33]

Raman spectroscopy was used to monitor both defect introduction and purity of the sample following the chemical treatment process, where the defect (D ~1320 cm^{-1}) and graphitic (G ~1590 cm^{-1}) bands are shown in Fig. 4. As the D band is activated by the presence of defects and edge planes, the I_D/I_G is often used to estimate the purity of SWNT samples, where a lower value generally represents a sample of higher purity.[34,35] Upon treatment with nitric acid a large increase of the I_D/I_G normally occurs, accompanied by a weakening of the RBM bands (100–400 cm^{-1}),[10] as small diameter SWNTs break apart to form carbonaceous impurities/fragments (rich in defects and edge planes).[8,11] Schaffer and co-workers have demonstrated that the I_D/I_G ratio of nitric acid treated HiPco SWNTs can be reduced after washing with sodium hydroxide, however, never reaching the level of the raw material.[4] This is in agreement with our recently published work.[2] Raman analysis of b-SWNTs shows an I_D/I_G ratio that is remarkably higher than that of r-SWNTs, which is attributable to the elevated quantity of non-carboxylated carbonaceous material left in the sample. Fig. 4 demonstrates that our chemical treatment not only reaches the level of the raw material, but surpasses it reducing the I_D/I_G of the o-SWNTs to approximately half of the value observed for the *r*-SWNTs (See supporting information Figure S7 for details†). This remarkable decrease in I_D/I_G was not observed for previously reported 2-step purified and oxidised SWNTs,[2] that on the contrary showed a raised value to almost double that of the raw material. In addition increased intensity of both the RBM and G^- bands of o-SWNTs, as well as sharpening of G-band components, indicate extensive removal of carbonaceous impurities.[36] AFM results also suggest that the sample is almost entirely comprised of SWNTs. Considering that XPS indicates partial conversion of sp^2 to sp^3 hybridised carbon and complete conversion of oxygenated functionalities to carboxylic acid groups during the chemical treatment, we can assume that the resultant D band is related to actual functionalisable defect sites present on the nanotube structure.

In order to investigate the effect of the chemical treatment on the electronic structure of the SWNTs, UV-Vis-NIR absorption and NIR-photoluminescence (NIR-PL) spectroscopies were carried out on all samples. The absorption spectrum of the r-SWNTs (Fig. 5 and 6A) is defined by a series of sharp optical/electronic transitions (van Hove singularities) attributable to the distribution of nanotube diameters and chiralities present in the sample.[37,38] Following nitric acid treatment (depending on reaction time and concentration) either a reduction in intensity or complete loss of van Hove singularities is normally observed due to degradation of nanotube structure, p-type doping effect, and the presence of carbonaceous fragments.[29,39–41] The o-SWNTs, however, demonstrate not only the persistence of the van Hove singularities (indicating preservation of electronic structure), but a significant enhancement in their intensity (Fig. 5 and 6A). This can be attributed to elimination of the spectral background associated with the carbonaceous impurities in the sample.[42] Additionally, the improved solubility displayed by o-SWNTs compared to the b-SWNTs (Figure S8, S9†) can be explained as a consequence of the introduction of functional groups on the nanotube surface.[43]

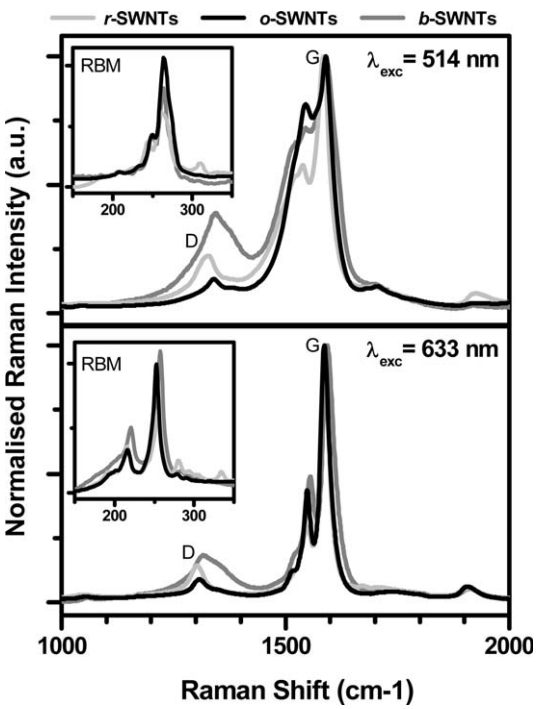

Fig. 4 Raman spectra of raw, oxidised and HNO_3/NaOH treated SWNTs with RBMs inset. All spectra have been normalised on the G-band.

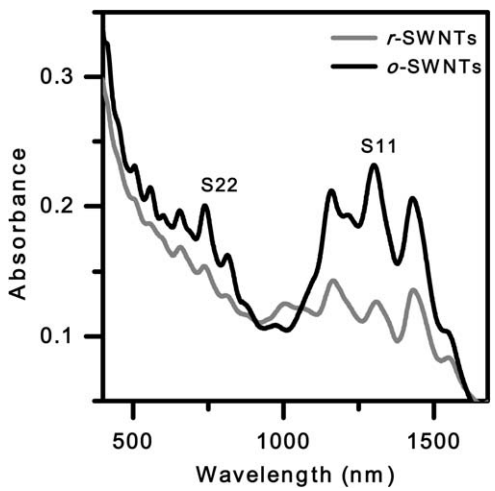

Fig. 5 UV-Vis-NIR absorption spectra of raw and oxidised SWNTs dispersed in NMP.

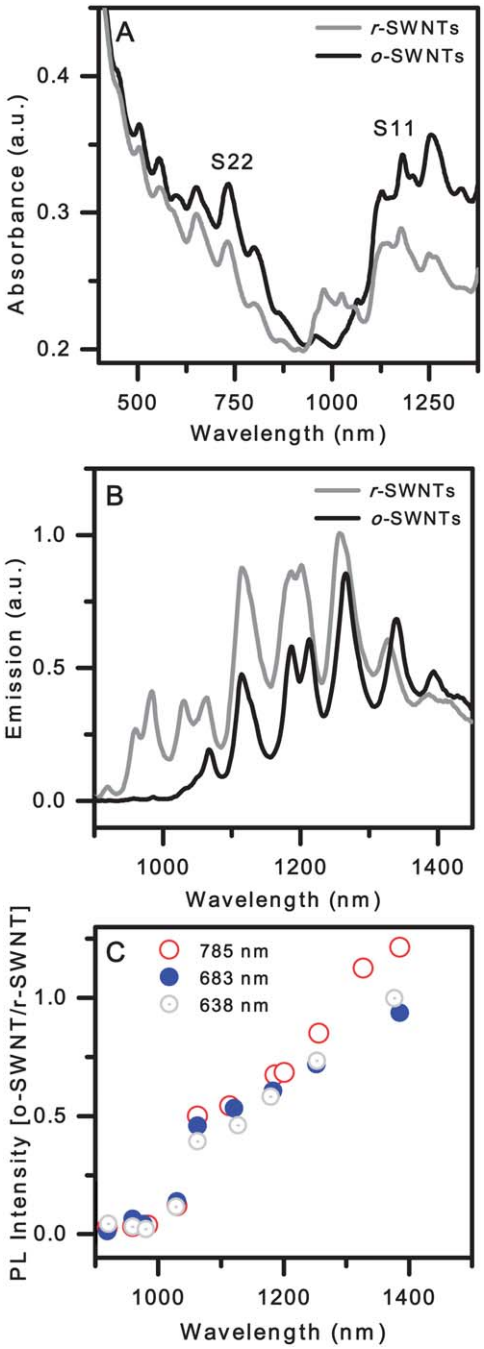

Fig. 6 Spectroscopy of raw and oxidised SWNTs. A) UV-Vis-NIR absorption spectra of SWNTs dispersed in aqueous SDBS, B) normalised NIR-PL spectra ($\lambda_{exc} = 785$ nm) of SWNTs dispersed in aqueous SDBS and C) NIR-PL intensity of the oxidised SWNTs relative to the raw SWNTs ($\lambda_{exc} = 638$, 683 & 785 nm).

The influence of the chemical treatment on the NIR-PL was investigated, as it is highly sensitive to defect introduction on the SWNT sidewalls.[44] The spectra of the r- and o- SWNTs are illustrated in Fig. 6B (emission intensity is normalised on the absorbance), and interestingly, relatively intense structured photoluminescence is still observed from the o-SWNTs, where the quenching of each band (900–1400 cm^{-1}) relative to the *r*-SWNTs, is displayed in Fig. 6C. A clear trend can be seen, where at shorter wavelength emission, greater quenching of the bands is demonstrated. Considering that the wavelength of the PL is related to the diameter[37] and hence the reactivity[9] of the SWNT, it is clear that the more reactive (shorter wavelength) nanotubes demonstrate greater quenching. This strongly indicates that greater numbers of defects are introduced onto the sidewalls of the smaller diameter SWNTs enhancing the possibility of non-radiative recombination of excited electron hole pairs.[44] Total loss of photoluminescence below 1050 nm, corresponding to diameters below approximately 0.9 nm, suggest destruction of the smallest SWNTs. This is in agreement with the disappearance of the small diameter contributions of the RBM band from the Raman spectra (Fig. 4). Photoluminescence is also observed from nanotubes subjected to HNO_3/NaOH treatment (Figure S9B†), however a greater quenching of larger diameter tubes is shown (Figure S9C†). This unexpected behaviour is still under investigation in our lab. The previously reported 2-step oxidised oo-SWNTs, also demonstrated persistence of their photoluminescent behaviour of nanotube materials following oxidation.[2] However a higher PL emission quenching was observed in the latter (90%), suggesting a much higher introduction of defects on the nanotube surface. Slight blue-shifts in the S_{11} van Hove maxima are accompanied by red-shifts in the emission bands (with no broadening) following the chemical treatment process (Table S2†). As the raw and oxidised samples are dispersed in an identical manner, this suggests a change in the band-gap structure of the semiconducting SWNTs,[45,46] which is an indication that the nanotubes displaying photoluminescence are chemically modified (oxidised) and not simply present as unreacted species in the sample.

Conclusions

We have developed a protocol for the preparation of high purity oxidised SWNTs, where carbonaceous impurities are removed with high efficiency and defects are effectively converted to functionalisable carboxylic acid groups. This protocol takes advantage of a short nitric acid oxidation treatment to minimise structural/electronic degradation of the SWNTs and sodium hydroxide treatments to remove carboxylated carbonaceous impurities. Essential to the purification, however, is the second oxidation step with hydrogen peroxide, which facilitates decomposition of the remaining carbonaceous impurities and full conversion of oxygenated functionality to carboxylic acid moieties. Importantly, the persistence of the characteristic optical properties of the SWNTs is demonstrated indicating preservation of the electronic structure. This procedure thus opens the door for the preparation of high purity, covalently functionalised SWNTs with minimal degradation of the unique electronic properties and hence enhances their potential for use in high-performance optical/electronic applications.

Acknowledgements

This work was supported by Science Foundation Ireland (PIYRA 07/YI2/I1052). The authors acknowledge the European Commission under framework 7 (PERG-GA-2009-249178), IRCSET and Intel (postdoctoral fellowship to IK and postgraduate scholarship to EDC) for support. We thank Dr Tatiana

Perova for granting access to Micro-Raman spectrometer, Dr Daniel Heller (MIT) for fruitful discussions, Dania Movia for technical support.

References

1 J. Chen, M. A. Hamon, H. Hu, Y. S. Chen, A. M. Rao, P. C. Eklund and R. C. Haddon, *Science*, 1998, **282**, 95–98.
2 E. Del Canto, K. Flavin, D. Movia, C. Navio, C. Bittencourt and S. Giordani, *Chem. Mater.*, 2011, **23**, 67–74.
3 E. Dujardin, T. W. Ebbesen, A. Krishnan and M. M. J. Treacy, *Adv. Mater.*, 1998, **10**, 611–613.
4 S. Fogden, R. Verdejo, B. Cottam and M. Shaffer, *Chem. Phys. Lett.*, 2008, **460**, 162–167.
5 H. Hu, B. Zhao, M. E. Itkis and R. C. Haddon, *J. Phys. Chem. B*, 2003, **107**, 13838–13842.
6 A. Jung, R. Graupner, L. Ley and A. Hirsch, *Phys. Status Solidi B*, 2006, **243**, 3217–3220.
7 J. Liu, A. G. Rinzler, H. J. Dai, J. H. Hafner, R. K. Bradley, P. J. Boul, A. Lu, T. Iverson, K. Shelimov, C. B. Huffman, F. Rodriguez-Macias, Y. S. Shon, T. R. Lee, D. T. Colbert and R. E. Smalley, *Science*, 1998, **280**, 1253–1256.
8 S. Nagasawa, M. Yudasaka, K. Hirahara, T. Ichihashi and S. Iijima, *Chem. Phys. Lett.*, 2000, **328**, 374–380.
9 T. J. Park, S. Banerjee, T. Hemraj-Benny and S. S. Wong, *J. Mater. Chem.*, 2006, **16**, 141–154.
10 C. G. Salzmann, S. A. Llewellyn, G. Tobias, M. A. H. Ward, Y. Huh and M. L. H. Green, *Adv. Mater.*, 2007, **19**, 883–887.
11 L. Shao, G. Tobias, C. G. Salzmann, B. Ballesteros, S. Y. Hong, A. Crossley, B. G. Davis and M. L. H. Green, *Chem. Commun.*, 2007, 5090–5092.
12 D. Tasis, N. Tagmatarchis, A. Bianco and M. Prato, *Chem. Rev.*, 2006, **106**, 1105–1136.
13 K. A. Worsley, I. Kalinina, E. Bekyarova and R. C. Haddon, *J. Am. Chem. Soc.*, 2009, **131**, 18153–18158.
14 E. Del Canto, K. Flavin, M. Natali, T. Perova and S. Giordani, *Carbon*, 2010, **48**, 2815–2824.
15 K. Flavin, K. Lawrence, J. Bartelmess, M. Tasior, C. Navio, C. Bittencourt, D. F. O'Shea, D. M. Guldi and S. Giordani, *ACS Nano*, 2011, **5**, 1198–1206.
16 V. Georgakilas, K. Kordatos, M. Prato, D. M. Guldi, M. Holzinger and A. Hirsch, *J. Am. Chem. Soc.*, 2002, **124**, 760–761.
17 M. S. Strano, C. A. Dyke, M. L. Usrey, P. W. Barone, M. J. Allen, H. W. Shan, C. Kittrell, R. H. Hauge, J. M. Tour and R. E. Smalley, *Science*, 2003, **301**, 1519–1522.
18 Z. Syrgiannis, B. Gebhardt, C. Dotzet, F. Hauke, R. Graupner and A. Hirsch, *Angew. Chem., Int. Ed.*, 2010, **49**, 3322–3325.
19 M. Prato, *Nature*, 2010, **465**, 172–173.
20 H. Yu, Y. G. Jin, F. Peng, H. J. Wang and J. Yang, *J. Phys. Chem. C*, 2008, **112**, 6758–6763.
21 P. Singh, S. Campidelli, S. Giordani, D. Bonifazi, A. Bianco and M. Prato, *Chem. Soc. Rev.*, 2009, **38**, 2214–2230.
22 A. Rinaldi, B. Frank, D. S. Su, S. B. A. Hamid and R. Schlögl, *Chem. Mater.*, 2011, **23**, 926–928.
23 G. Tobias, L. Shao, B. Ballesteros and M. L. H. Green, *J. Nanosci. Nanotechnol.*, 2009, **9**, 6072–6077.
24 I. Horcas, R. Fernández, J. M. Gómez-Rodríguez, J. Colchero, J. Gómez-Herrero and A. M. Baro, *WSXM: A software for scanning probe microscopy and a tool for nanotechnology*, AIP, 2007.
25 D. Bonifazi, C. Nacci, R. Marega, S. Campidelli, G. Ceballos, S. Modesti, M. Meneghetti and M. Prato, *Nano Lett.*, 2006, **6**, 1408–1414.
26 C. l. Bergeret, J. Cousseau, V. Fernandez, J.-Y. Mevellec and S. Lefrant, *J. Phys. Chem. C*, 2008, **112**, 16411–16416.
27 J. Zhang, H. Zou, Q. Qing, Y. Yang, Q. Li, Z. Liu, X. Guo and Z. Du, *J. Phys. Chem. B*, 2003, **107**, 3712–3718.
28 A. G. Rinzler, J. Liu, H. Dai, P. Nikolaev, C. B. Huffman, F. J. Rodríguez-Macías, P. J. Boul, A. H. Lu, D. Heymann, D. T. Colbert, R. S. Lee, J. E. Fischer, A. M. Rao, P. C. Eklund and R. E. Smalley, *Appl. Phys. A: Mater. Sci. Process.*, 1998, **67**, 29–37.
29 W.-B. Liu, S. Pei, J. Du, B. Liu, L. Gao, Y. Su, C. Liu and H.-M. Cheng, *Adv. Funct. Mater.*, 2011, **21**, 2330–2337.
30 B. Ballesteros, G. Tobias, L. Shao, E. Pellicer, J. Nogués, E. Mendoza and M. L. H. Green, *Small*, 2008, **4**, 1501–1506.
31 M. Holzinger, A. Hirsch, P. Bernier, G. S. Duesberg and M. Burghard, *Appl. Phys. A: Mater. Sci. Process.*, 2000, **70**, 599–602.
32 B. J. Landi, C. D. Cress, C. M. Evans and R. P. Raffaelle, *Chem. Mater.*, 2005, **17**, 6819–6834.
33 M. A. Hamon, J. Chen, H. Hu, Y. S. Chen, M. E. Itkis, A. M. Rao, P. C. Eklund and R. C. Haddon, *Adv. Mater.*, 1999, **11**, 834–840.
34 M. S. Dresselhaus, G. Dresselhaus, R. Saito and A. Jorio, *Phys. Rep.*, 2005, **409**, 47–99.
35 M. Lazzeri, S. Piscanec, F. Mauri, A. C. Ferrari and J. Robertson, *Phys. Rev. B: Condens. Matter Mater. Phys.*, 2006, **73**, 155426.
36 U. J. Kim, C. A. Furtado, X. Liu, G. Chen and P. C. Eklund, *J. Am. Chem. Soc.*, 2005, **127**, 15437–15445.
37 S. M. Bachilo, M. S. Strano, C. Kittrell, R. H. Hauge, R. E. Smalley and R. B. Weisman, *Science*, 2002, **298**, 2361–2366.
38 R. Saito, G. Dresselhaus and M. S. Dresselhaus, *Phys. Rev. B: Condens. Matter*, 2000, **61**, 2981–2990.
39 Y. Q. Liu, L. Gao, J. Sun, S. Zheng, L. Q. Jiang, Y. Wang, H. Kajiura, Y. M. Li and K. Noda, *Carbon*, 2007, **45**, 1972–1978.
40 S. R. C. Vivekchand, R. Jayakanth, A. Govindaraj and C. N. R. Rao, *Small*, 2005, **1**, 920–923.
41 Y. Q. Xu, H. Q. Peng, R. H. Hauge and R. E. Smalley, *Nano Lett.*, 2005, **5**, 163–168.
42 M. E. Itkis, D. E. Perea, S. Niyogi, S. M. Rickard, M. A. Hamon, B. Zhao and R. C. Haddon, *Nano Lett.*, 2003, **3**, 309–314.
43 N. Karousis, N. Tagmatarchis and D. Tasis, *Chem. Rev.*, 2010, **110**, 5366–5397.
44 L. Cognet, D. A. Tsyboulski, J. D. R. Rocha, C. D. Doyle, J. M. Tour and R. B. Weisman, *Science*, 2007, **316**, 1465–1468.
45 S. Ghosh, S. M. Bachilo, R. A. Simonette, K. M. Beckingham and R. B. Weisman, *Science*, 2010, **330**, 1656–1659.
46 S. H. Qin, D. Q. Qin, W. T. Ford, J. E. Herrera, D. E. Resasco, S. M. Bachilo and R. B. Weisman, *Macromolecules*, 2004, **37**, 3965–3967.